ELSEVIER

Microelectronics Journal 30 (1999) 1149–1154

Microelectronics Journal

www.elsevier.com/locate/mejo

Design and fabrication of metal bolometers on high porosity silicon layers

L. Boarino[a,*], E. Monticone[a], G. Amato[a], G. Lérondel[a], R. Steni[a], G. Benedetto[a], A.M. Rossi[a], V. Lacquaniti[a], R. Spagnolo[a], V. Lysenko[b], A. Dittmar[b]

[a]*Istituto Elettrotecnico Nazionale Galileo Ferraris, Thin Film Lab, Strada delle Cacce 91, I-10135 Turin, Italy*
[b]*Laboratory of Materials Physics, INSA de Lyon, CNRS UMR 5511, 20, Av. Albert Einstein, Bat. 502. 69621, Villeurbanne Cedex, France*

Abstract

Fabrication and characterisation of metal bolometers on p-type porous silicon (PS) layers are presented as an alternative to more complex micromachining processes for thermal insulation of sensors. A comparison of Nb strips deposited on layers of PS of varying thicknesses and porosities and on other substrates such as amorphous glass and crystalline silicon is described. Results of electrical characterisation, photoacoustic depth profiling and FEM thermal analysis are presented. Photoacoustic investigation on very high porosity layers (≥90%) gives promising indications on the thermal insulation efficiency of thin PS layers, which could be competitive with suspended structures for their low cost and number of fabrication steps.

Keywords: Metal bolometers; FEM thermal analysis; p-Type porous silicon (PS)

1. Introduction and problem statement

Metal film bolometers are extensively used in a variety of fields, from IR imaging to medical equipment, metrology and industrial applications, due to the wide flat frequency response (from near to far IR, 0.8–400 μm), low costs and room temperature operation.

The resistance, R, of a metal film bolometer changes with an incident optical power, P, as

$$R = R_0(1 + \alpha P/G)(1 - \alpha I_b^2 R_0 G^{-1})^{-1} \quad (1)$$

where $\alpha = R^{-1}\mathrm{d}R/\mathrm{d}T$ and is the temperature coefficient of resistance, I_b is the bias current and G the thermal conductance of the bolometer. In the case of metal films $\alpha > 0$, so the current must be $I_b < \sqrt{G/\alpha R_0}$ to avoid self-heating.

An important figure of merit for a bolometric sensor is the responsivity S defined as voltage change δV of the bolometer with respect to the incident power P,

$$S = \frac{\delta V}{P} = \eta I_b \alpha R G(f)^{-1} \quad (2)$$

where η(is the efficiency and $G(f)$ can be expressed as, $G(f) = G_s(f)\sqrt{1 + (2\pi f C/G_s(f))^2}$ where $G_s(f)$, the film/substrate thermal conductance is defined as $G_s(f) = k_s\sqrt{2\pi k_s A(1 + \sqrt{2Af/D_s + Af/D_s})}$, with C thermal capacitance of the substrate, A the bolometer area and D_s the thermal diffusivity of the substrate. The responsivity is affected by the thermal conductance to the substrate in the frequency range ($2D_s/A \ll \delta \ll G_s/C$), where $\tau_s = A/2D_s$ is the effective time constant and $S \propto f^{-1/2}$. In the regime in which $f \gg 2D_s/A$, $S \propto f^{-1}$, and the time constant is $\tau_E = C/G(0)$, typical of a lumped bolometer.

In the past, bulk and surface micromachining processes have been used to reduce thermal conductance towards the substrate [1,2] increasing the efficiency of sensors, but both methods are affected by some drawbacks. For the bulk processes, like KOH and TMAH anisotropic etching, possible disadvantages are a low compatibility with standard CMOS microelectronic processes, greater area consumption, requirement of double alignement, fragility of the suspended structures and time consuming processes. For the surface micromachining the limit is generally represented by the small depth of air gaps obtainable removing the sacrificial layers.

2. Solution

Porous silicon (PS) exhibits interesting thermal properties as a new material for thermal insulation of sensors and devices [3,4]. Like the wide ranging photoluminescence properties [5], also its thermal conductivity ranges from the crystalline silicon value ($1.48\ \mathrm{W\,K^{-1}\,cm^{-1}}$) to less than three orders of magnitude lower, depending on the porosity and silicon crystallite sizes [6,7]. Such results

* Corresponding author. Tel.: + 39-011-3919-627; fax: + 39-011-3919-621.

0026-2692/99/$ - see front matter
PII: S0026-2692(99)00078-6

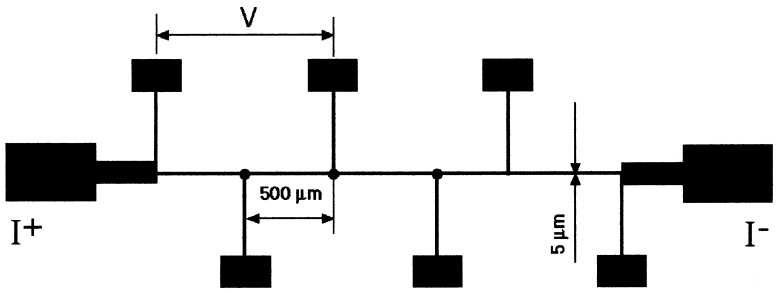

Fig. 1. Measurement configuration used to determine $G(0)$.

open new possibilities for the realisation of structures and processes for thermal insulation.

The use of a silicon technology compatible substrate gives the well known advantages of area reduction and photolithographic processing for multiple sensors and arrays.

PS micromachining has been successfully used as a sacrificial layer for bridges and suspended structures for radiation and flux sensors, giving origin to air gaps up to 80–100 μm, after a light oxidisation of the PS layer and its removal in HF [8]. Among the several applications of porous silicon, one of the most promising is the possibility to realise a low thermal conductance PS layer of desired thickness, without any suspended structure and layer removal, so mantaining the planarity, giving a better mechanical stability, reducing times, number of steps and costs of the fabrication process. This solution should result in a very effective thermal insulation of arrays of thermal and gas sensors.

PS is obtained by electrochemical anodisation of bulk Si in HF-based solutions. Varying HF title and current density during anodization, well defined layer thicknesses with different porosities can be obtained, which are suitable for fabrication of optical devices like Bragg reflectors and Fabry–Perot filters: see for a review Ref. [9]. A variety of morphologies, depending on the substrate doping, is obtainable, with thicknesses ranging from tens of nanometers to hundreds of micrometers, and porosity varying from 20 to 80% and more [10–14]. The silicon wires and structures also vary from the scale of micrometers to few nanometers with well proved crystallinity.

All the physical properties of PS are strongly affected by porosity (pores/structures ratio), and the resulting material behaves like a homogeneous medium with characteristics determined by porosity and structure dimensions. PS material is classified in three categories: macroporous silicon (n-type, structures size from micrometers to 50 nm), mesoporous (p+, n+, between 50 nm and 2 nm), and nanoporous silicon (p-type, crystallites size <2 nm).

Very low thermal conductivity is observed in these materials when crystallites size becomes comparable with phonon mean free path (43 nm in c-Si) [15]. In particular, p-type PS reveals strong similarity with a well known low thermal conductivity material: the silica aerogel systems. Morphology, and results of several characterisation techniques give indication that aerogel and PS thermal behaviour is based on the same physical phenomena.

3. Fabrication

PS layers of different porosity and thickness were produced in order to study the effect of morphology and PS preparation conditions on the thermal insulation performance. The use of p-type substrate allows the highest porosity ranges respect to other doping. ⟨100⟩ oriented samples 4–6 Ω cm resistivity have been electrochemically anodised in 15–35% HF, water and ethanol, with current density ranging from 20 to 162 mA cm^{-2}, following the conditions outlined in previous work [16]. The layer thickness obtained by these conditions range from 2 to 48 μm with porosity varying from 50 to 90%. On 90% PS layer, freeze drying has been applied to avoid cracking due to capillary tensions.

For all the samples a good compromise between thickness, porosity and surface flatness must be reached, to avoid the well known chemical dissolution phenomena occurring in p-type PS for long anodisation time [17]. When this effect is negligible, the PS surface flatness is the same of c-Si polished wafers. SEM analysis shows good isotropy and homogeneity of the porous structure and thickness layers.

Niobium bolometers have been fabricated on few PS layers, taking advantage of the high temperature coefficient of resistance, low thermal conductance, mechanical properties and low frequency noise of this material. First results of electrical characterisation are here reported for two devices deposited on 65 and 70% porosity, while realisation of other devices is still in progress on higher porosity substrates.

Nb films were deposited by rf magnetron sputtering at a base pressure of 4×10^{-5} Pa. The film thickness was inferred from deposition rates and checked by Alpha-step measurements within an error of 10% of the nominal value.

The bolometer strips were realised using a standard photolithographic procedures and a RIE etching in CF_4 but for some samples the geometry was defined by lift-off. Between the metallic film and the underlying PS a layer of thermally evaporated SiO_x (200 nm thick) was interposed to ensure an adequate electrical insulation of the metallic film

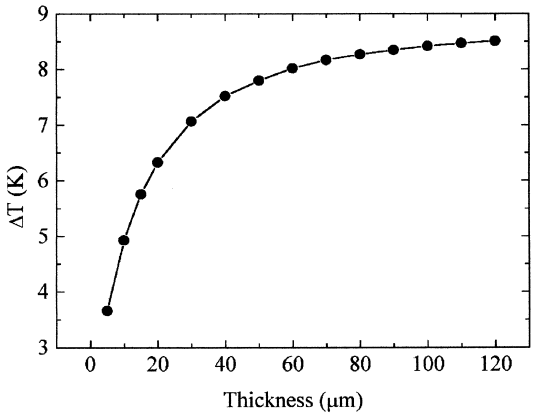

Fig. 2. Temperature changes due to electrical power dissipated in the bolometer strip as calculated by FEM analysis.

from the Si substrate and to protect PS surface from the RIE process and the alkaline photoresist developer of the photolithographic process as the CF_4 etching rate for PS is at least 100 times larger than for Nb films.

4. Characterisation results

Two methods have been used to determine the thermal parameters of the strips: the resistive heating method, where the bolometer is biased with a constant current and data are acquired by a PC, and the bolometric method where a pulsed laser diode beam is focused on the bolometer ($\lambda = 693$ nm). The voltage response to a constant current is then recovered by a lock-in amplifier. From Eq. (1), the thermal conductance $G(0)$ can be obtained from the measurement of the bolometer resistance R as a function of the biasing current I_b.

Using the configuration of Fig.1, the thermal conductance $G(0)$ has been measured for a 50 nm Nb film on amorphous glass and on PS, as a function of the strip area A. With $\alpha \sim 0.0021$, the transfer coefficient defined as $h_c = G(0)/A$, for glass has a constant value of $h_c = 7\ \mathrm{W\ K^{-1}\ cm^{-2}}$, for PS is $2.5–5\ \mathrm{W\ K^{-1}\ cm^{-2}}$. With the aim to estimate the temperature dependence of the bolometer on the PS thickness, a FEM simulation of a device realised on a 6" silicon wafer (700 μm thick) with a porous layer of 65% porosity has been undertaken.

Fig. 2 indicates the temperature change due to electrical power dissipated in the bolometer strip. The temperature variation increases quickly up to 30 μm, with a saturation after 60–70 μm.

The response of the device on PS 48 μm thick is about 90% of an equivalent device deposited on a substrate of infinite thickness with the same conductivity. Knowing the thermal conductivity of the amorphous glass, ($0.011\ \mathrm{W\ K^{-1}\ cm^{-1}}$) a direct comparison between the two bolometers gives the PS layer thermal conductivity, ranging from 0.004 to $0.008\ \mathrm{W\ K^{-1}\ cm^{-1}}$.

Measurements on higher porosity sample (70%) reveal almost the same thermal conductance values of glass and 65% PS, in spite of the lower thickness (8 μm). This gives indication that this PS layer has lower thermal conductivity values. With the mentioned values of thermal conductivity, a steady state responsivity of the sensor of 50 V/W ($I_b =$ 7.6 mA) has been evaluated, close to that of bolometers on SiO_2 membranes [18]. In Fig. 3 the voltage response of a bolometer on PS ($I_b = 0.1$ mA) is shown. Interpolation of data in Fig. 3 using Eq. (2) gives the time constant $\tau_E = C/G = 0.3$ ms, due to the thermal capacitance of the bolometer.

From $\tau_s = A/2D_s$ it is then possible to evaluate a thermal diffusivity for PS of $3.5 \times 10^{-3}\ \mathrm{cm^{-2}\ s^{-1}}$ [7].

These values are in good agreement with recent results of photoacoustic depth profile (PA) on the same material. The experimental apparatus and the theoretical model adopted has been described in more detail previously [19]. Photoacoustic depth profile has been succesfully applied to the nondestructive evaluation of thermal properties of

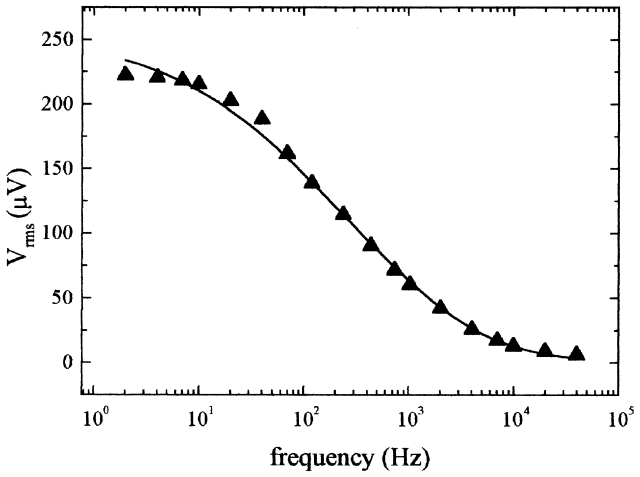

Fig. 3. Theoretical and experimental voltage response of a bolometer on PS ($I_b = 0.1$ mA) as a function of the modulation frequency.

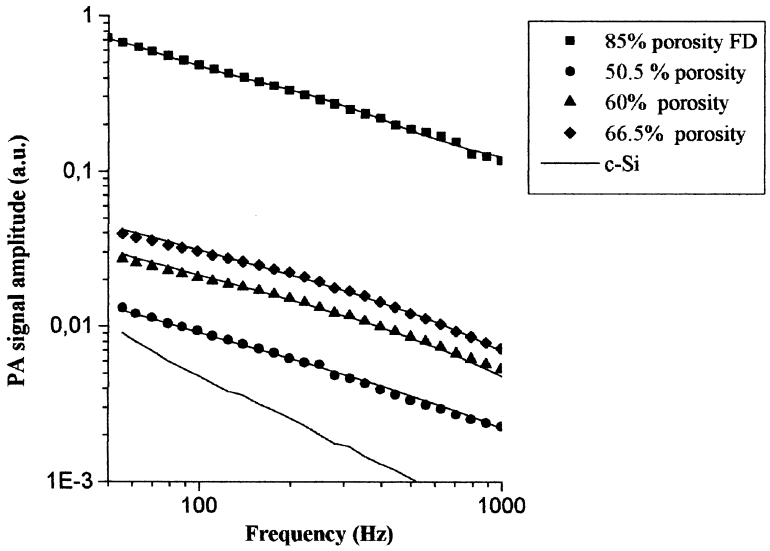

Fig. 4. Amplitude of PA signal for crystalline silicon and PS layers with different increasing porosity. Sample with 90% porosity has been freeze-dried after preparation.

materials, like thermal diffusivity and conductivity. With a good control of the realisation parameter of PS, this technique becomes quantitative with an immediate response.

In PA depth profile thermal waves are generated by modulated light absorption and propagate inside the material. PA signal is proportional to the surface temperature of a sample, offering the possibility to evaluate the thermal properties like diffusivity and conductivity. Scanning the modulation frequency gives the possibility to probe the thermal response of layers closer and closer to the surface. Using crystalline silicon as a reference, the thermal mismatch due to the PS insulating layer is evidenced. By a curve fitting procedure the thermal diffusivity can be evaluated.

Fig. 4 shows the experimental and theoretical curves of PA signal amplitude vs. modulation frequency, for PS samples of different porosity. The squares represents experimental PA signal of a PS layer with 90% porosity obtained by freeze-drying method, to avoid cracking due to capillary tensions during drying. The estimated thermal conductivity, also confirmed by 3ω measurements [7] is $0.0005\ \mathrm{W\,K^{-1}\,cm^{-1}}$.

In the case of one of the PS layers used as a thermal insulating substrate for bolometers, the thermal conductivity value obtained by fitting the PA signal amplitude vs. modulation frequency is $0.0039\ \mathrm{W\,K^{-1}\,cm^{-1}}$. This is in good agreement with the data obtained by electrical measurements. To explain the occasional drastic difference among thermal conductivity values of PS published in literature [20], it should be stated that porosity is a quite rough and

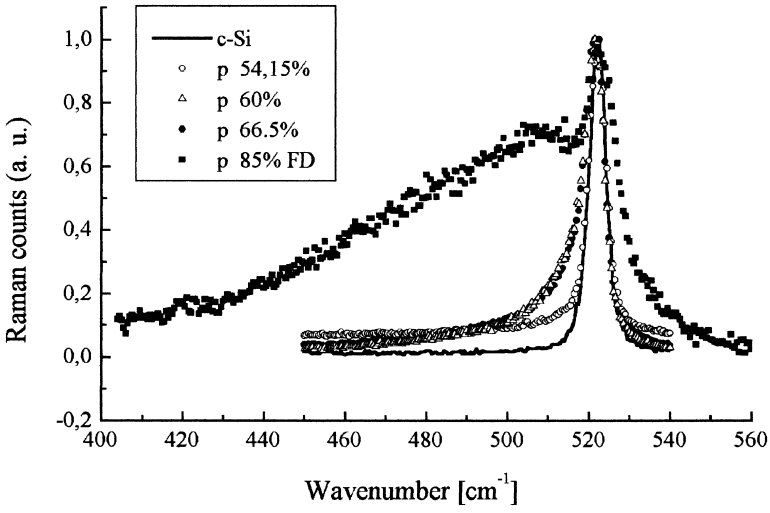

Fig. 5. Raman spectra of PS sample p-type ⟨100⟩, 4–6 Ω cm, of different porosity: a red shift and a broadening of the peak is evident from increasing porosity, due to the phonon confinement.

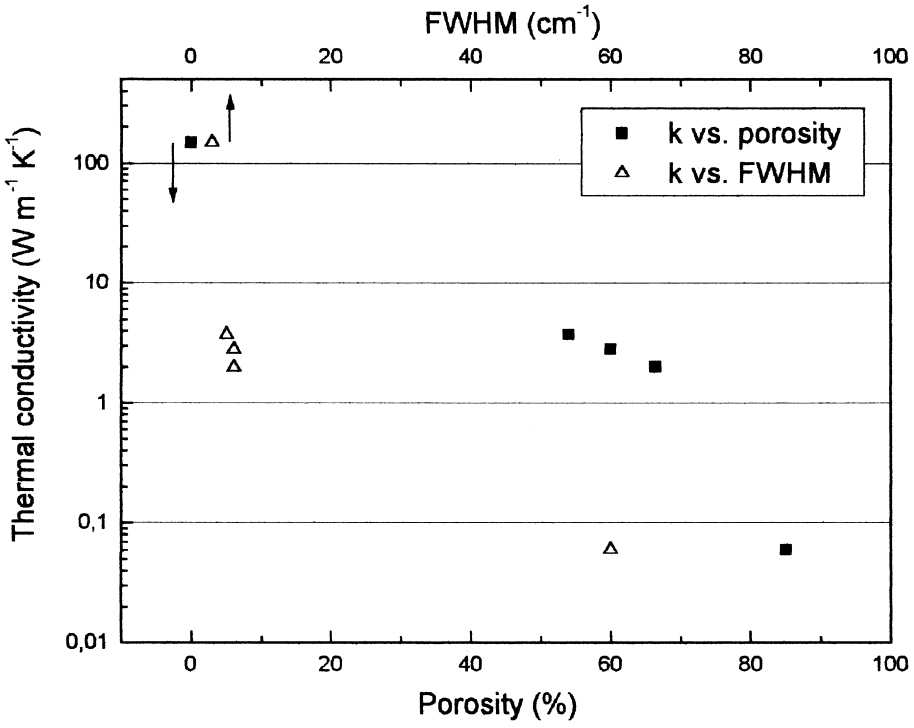

Fig. 6. Thermal conductivity k as a function of porosity (lower x-axis) and FWHM (full width half maximum) (top x-axis): a decay of k for 90% porosity and for FWHM of 60 cm^{-1} is observable.

ambiguous parameter to describe the physical properties of this material. Morphology and structure size can differ completely depending on the preparation procedures and wafer doping. Furthermore, current models of heat propagation in microstructures are based on phonon mean free path and structure size. Raman spectroscopy can give in this case a crucial information on crystallite dimension by means of a detailed lineshape analysis [21].

Raman spectra of the p-type PS layers characterised by photoacoustic depth profiling are shown in Fig. 5. A progressive red shift and broadening of the Raman peak is evident for samples of increasing porosity. Plotting thermal conductivity k vs. porosity and FWHM (full width half maximum) a decay of k for 90% porosity and for FWHM of 60 cm^{-1} is observable (Fig. 6). The FWHM is directly connected to the structure size under 20 nm, so the effect of phonon confinement appears for crystallite sizes minor than 42 nm (phonon mean free path in bulk silicon) and becomes stronger when silicon structures reduce to few nanometers.

5. Conclusions

Fabrication and characterisation of room temperature Nb film bolometers deposited on highly porous silicon layers has been reported, whose responsivity and time constant have been evaluated from electrical heating and bolometric method (50 V W^{-1} and 4 ms). These first results show the possibility to use a massive PS layer instead of surface or bulk micromachining processes. For the devices studied up to now, the efficiency of PS as a thermal insulator is the same as that of amorphous glass, and the higher porosity sample (70%) allows a minimum layer thickness of 8 μm.

A detailed PA characterisation confirms the results obtained from the bolometers and gives indications for further improvements in the efficiency of the devices: PA characterisation of 90% porosity material requiring freeze-drying method indicates very low thermal conductivity values (5×10^{-4} W K^{-1} cm^{-1}), opening the perspective to use thinner PS layers (<8 μm). Further improvement of bolometer performance is also expected using better absorbing materials.

References

[1] K.E. Petersen, Proceedings of the IEEE 70 (1982) 5.
[2] H. Guckel, J.J. Sniegowski, T.R. Christenson, S. Mohney, T.F. Kelly, Sensors and Actuators 20 (1989) 117.
[3] A. Drost, P. Steiner, H. Moser, W. Lang, Sensorsand Materials 7 (1995) 111.
[4] V. Lysenko, P. Roussel, G. Delhomme, V. Rossokhaty, V. Strikha, A. Dittmar, D. Barbier, N. JaffrezicRenault, C. Martelet, Sensors and Actuators A 67 (1-3) (1998) 205.
[5] L.T. Canham, Applied Physics Letters 57 (10) (1990) 1046.
[6] G. Benedetto, L. Boarino, N. Brunetto, A. Rossi, R. Spagnolo, G. Amato, Philosphical Magazine B 76 (3) (1997) 383–393.
[7] G. Gesele, J. Linsmeier, V. Drach, J. Fricke, R. Arens-Fischer, Journal of Physics D: Applied Physics 30 (1997) 2911–2916.
[8] W. Lang, in: G. Amato, C. Delerue, H.J. von Bardeleben (Eds.),

Structural and Optical Properties of Porous Silicon Nanostructures, Gordon and Breach, London, 1997, pp. 597.
[9] M. Thoenissen, M. Krueger, G. Lérondel, R. Romestain, chap. 12.2, in: L. Canham (Ed.), Properties of Porous Silicon, Emis Datareview Series 18 INSPEC Editions, 1992, pp. 349.
[10] R.L. Smith, S.D. Collins, Journal of Applied Physics 71 (8) (1992) R1.
[11] G. Amato, N. Brunetto, Porous silicon via freeze drying, Materials Letters 26 (1996) 295.
[12] O. Belmont, D. Bellet, Y. Bréchet, Journal of Applied Physics 79 (1996) 7586.
[13] J. Von Behren, P.M. Fauchet, E.H. Chimowitz, C.T. Lira, Materials Research Society Symposium Proceedings 452 (1997) 565.
[14] L.T. Canham, A.G. Cullis, C. Pickering, O.D. Dosser, T.I. Cox, P. Lynch, Nature (London) 368 (1994) 133.
[15] G. Chen, Journal of Heat Transer 118 (1996) 539.
[16] G. Lérondel, P. Ferrand, R. Romestain, MRS Symposium Proceedings 452 (1996) 711–716.
[17] A. Halimaoui, in: J.C. Vial, J. Derrien (Eds.), Porous Silicon Science and Technology, Les Editions de Physique, Springer, Berlin, 1994, pp. 33.
[18] S.S. Jin, K.W. Ping, Sensors and Actuators A 33 (1992) 183.
[19] G. Benedetto, L. Boarino, R. Spagnolo, Applied Physics A 64 (1997) 155–159.
[20] W. Lang, Thermal conductivity of porous silicon, in: L. Canham (Ed.), Properties of Porous Silicon, INSPEC, London, 1997, pp. 138.
[21] N. Brunetto, G. Amato, Thin Solid Films 297 (1997) 122–124.